DECONVOLUTION OF UPGOING AND DOWNGOING WAVEFIELDS: A DATA EXAMPLE FROM THE UTSIRA OBN SURVEY

T. Seher[1], Y. Ren[1], H. Masoomzadeh[1], T. Degel[1], E. Cho[1], M. Hawke[1], S. Baldock[1]

[1] TGS

Summary

Both number and size of OBN surveys have been increasing in recent years. This requires efficient processing solutions for both demultiple and deghosting to prepare the seismic data for imaging. One approach that meets this requirement is up-down wavefield separation of the hydrophone and geophone records followed by up/down deconvolution or downgoing wavefield deconvolution. The combination of wavefield separation and deconvolution attenuates free surface effects and removes the source signature.

In this study, we demonstrate that up/down deconvolution and downgoing wavefield deconvolution can be implemented in a single processing flow, which simplifies the processing sequence required for imaging with both the up- and downgoing wavefields. This simplification greatly reduces human effort and processing turn-around. In addition, the combination of the two techniques allows the construction of complimentary images from both wavefields. Most importantly, the mirror image using the downgoing wavefield offers superior resolution in the shallow subsurface, which may have significant impact for the characterization of shallow targets.

Deconvolution of upgoing and downgoing wavefields: A data example from the Utsira OBN survey

Introduction

Both number and size of multi-component ocean bottom node (OBN) surveys have been growing constantly over the last years. The increase in survey size requires more efficient processing solutions because some data preconditioning steps such as demultiple and deghosting can become costly for larger surveys. A key advantage of multi-component seismic data is the possibility of separating the data into up- and downgoing wavefields (Wang et al., 2010). This separation in turn enables the attenuation of free surface effects such as multiples and ghosts using up/down deconvolution (UDD) (Sonneland & Berg, 1987; Amundsen, 1993, 2020; Ziolkowski et al., 1999) and downgoing wavefield deconvolution (DGD) (Lokshtanov, 2005, 2021; Hampson & Szumski, 2020; Caprioli & Kristiansen, 2021). These techniques, which are attractive due to their simplicity, allow high quality imaging using either conventional imaging for the UDD results or mirror imaging for the DGD data.

While the geophysical foundation for UDD and DGD is well established (Amundsen, 1993; Lokshtanov, 2005), the recent studies by Hampson and Szumski (2020) have sparked a renewed interest in deconvolution methods for the downgoing wavefield. In this study, we demonstrate how DGD can be implemented using minor modifications to the UDD processing flow. The combination of wavefield separation, UDD and DGD in a single processing step allows a simplification of the processing sequence, which reduces human effort and production turnaround. As a by-product, DGD combined with mirror imaging delivers superior images of the shallow subsurface compared to the UDD results.

In this paper, we first describe the wavefield separation processing flow with a particular focus on UDD and DGD. We then demonstrate the effectiveness of our processing solution using a synthetic data example. Later we apply the method to a subset of the Utsira survey of the South Viking Graben. We use this field data example to demonstrate the advantages of applying mirror imaging to DGD data. Finally, we finish with a discussion and conclusion.

Method

Multi-component seismic data are usually processed using two separate flows. In the first flow, the hydrophone and vertical geophone data are separated below the seafloor into up- and downgoing wavefields. This process is followed by source deghosting and demultiple. In the second flow, the wavefields are separated above the seafloor followed by UDD (Wang et al., 2010). Therefore, preparing the up- and downgoing wavefields for imaging requires at least two separate processing flows (Figure 1a). We have implemented UDD and DGD inside a single processing sequence. This simplified approach only requires a single processing flow, which reduces the complexity of the processing sequence (Figure 1b).

Both UDD and DGD effectively attenuate free surface multiples/ghosts and deconvolve the source signature. UDD is commonly implemented as a spectral division in the frequency domain. The earth impulse response X at the seafloor is estimated as the ratio of upgoing wavefield U and downgoing wavefield D:

$$X = UD^*/(DD^* + \varepsilon^2) \ . \qquad (1)$$

Here, ε is a stabilization parameter. For comparison, DGD estimates the redatumed impulse response ZX from the downgoing wavefield D, the source wavefield S and the sea surface reflectivity R:

$$RZX = (D - S)D^*/(DD^* + \varepsilon^2) \ . \qquad (2)$$

Here, Z is the round-trip operator in the water layer. In our algorithm, we have implemented two methods for estimating the source wavefield S. The first method mutes the downgoing wavefield D around the direct wave (Hampson & Szumski, 2020). This approach does not require knowledge about the upgoing wavefield. The second method estimates the source wavefield using the cross-ghosting method (Soubaras, 1996; Hampson & Szumski, 2020), which needs both the up- and downgoing wavefields. While the first method is well suited for deep water surveys, the second method is appealing for shallow water surveys, where the source bubble interferes with subseafloor reflections.

To test these new algorithms, we have created a synthetic multicomponent dataset for a 1D velocity model using finite difference modelling. These modelled hydrophone and vertical geophone records are transformed into the τ-p domain, where the data are calibrated using the cross-ghosting technique (Soubaras, 1996) and separated into up- and downgoing wavefields (Figure 2a-d). While this step attenuates the receiver side multiples, the source side multiples and ghost, as well as the source signature remain in the data. This remaining energy can be removed using either UDD or DGD (Figure 2e&f). While UDD places the receivers at the seafloor, DGD places the receivers at the mirror location. This explains the time delay between the two deconvolution results.

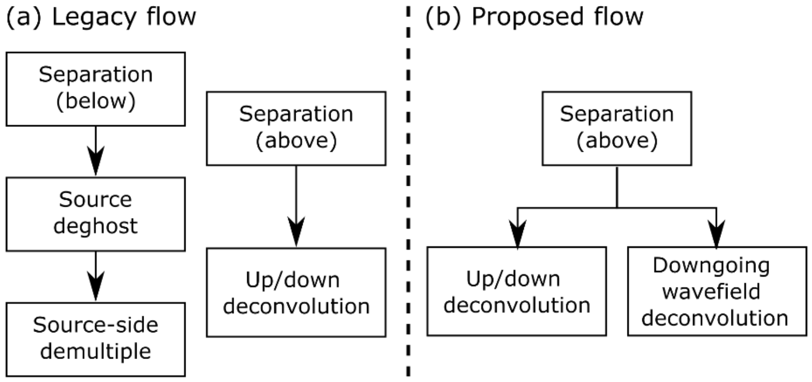

Figure 1 *Legacy and proposed processing flows for wavefield separation (adapted from Wang et al., 2010).*

Examples

To compare the effects of UDD and DGD on seismic imaging, we applied our new solutions to a subset of the Utsira survey of the South Viking Graben. The test dataset comprised a total of 611 multi-component receivers spaced 50 m apart along a single receiver line and shots in 3D shot carpet. The data preparation involved shear wave noise attenuation as well as shot carpet regularization to a regular grid of 12.5 m by 12.5 m. The wavefield separation workflow is identical to the one described for the synthetic data example above.

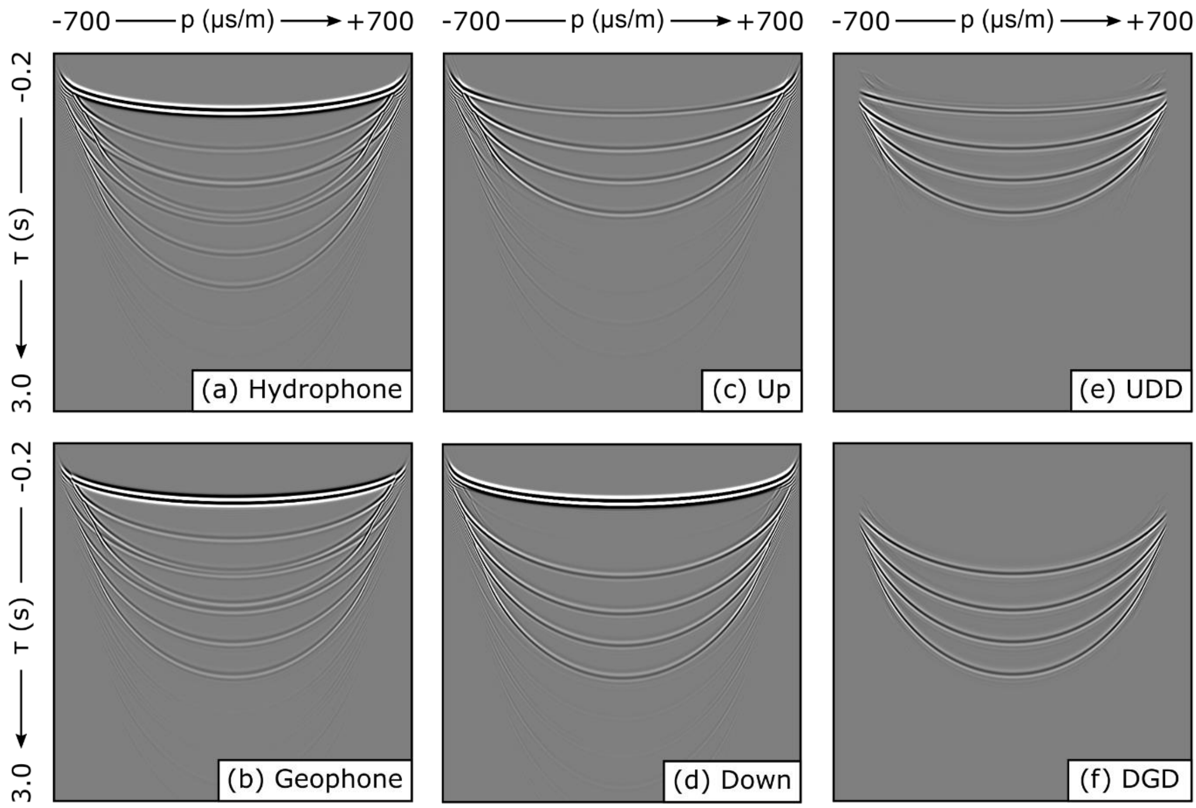

Figure 2 *Synthetic data example showing the results of UDD and DGD in the τ-p domain. The figures show a single slice through the full τ-p_x-p_y volume at p_y=0. Figures a-d have a different dynamic range than figures e&f.*

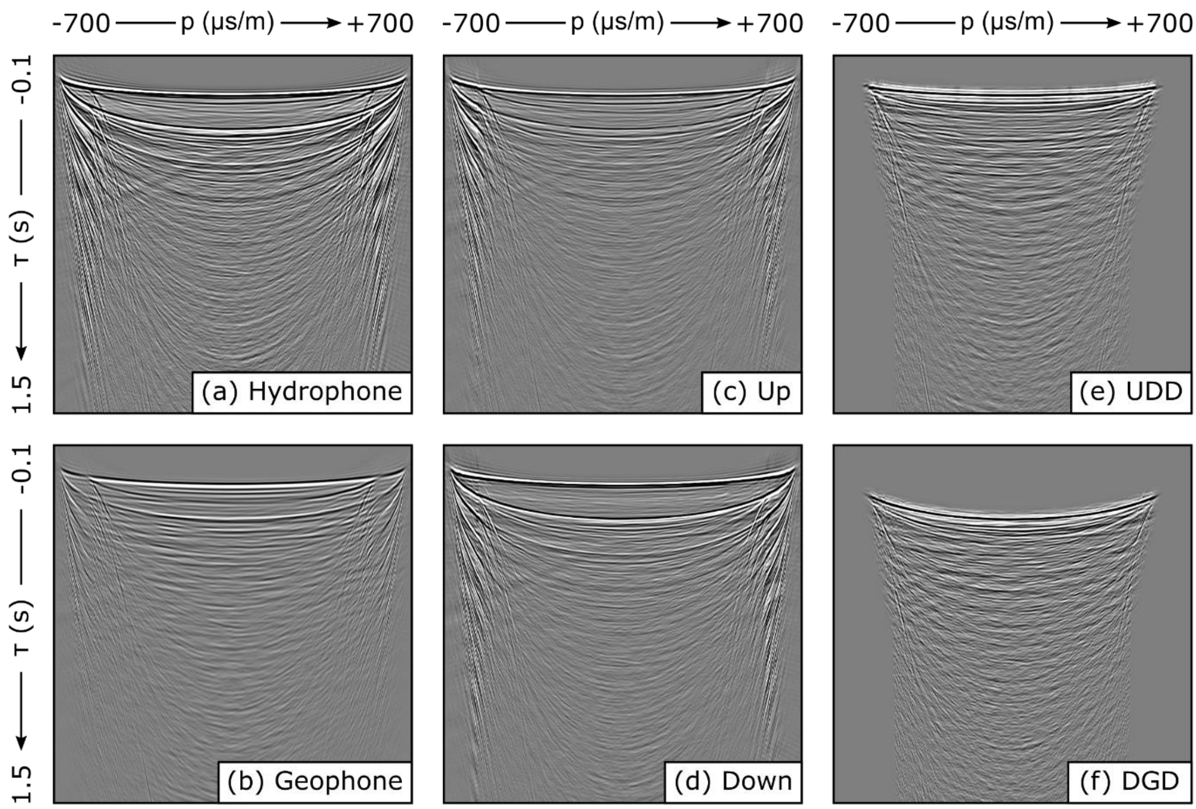

Figure 3 *Field data example in the τ-p domain showing the processing steps required to prepare the data for imaging including UDD and DGD. These figures show a single slice through the full* τ-p_x-p_y *volume at* $p_y=0$*. Figures a-d have a different dynamic range than figures e&f.*

The results of applying our wavefield separation workflow to the up- and downgoing wavefield for a single receiver are shown in Figure 3. Examining the downgoing wavefield (Figure 3d) shows that our wavefield separation process has successfully attenuated the upgoing energy between the direct wave and the first order multiple. Comparing the UDD and DGD results (Figure 3e&f) shows similar wavefields apart from a time delay due to the water column round-trip.

Finally, we applied wavefield separation followed by UDD and DGD for all receivers from our test line. Next, we applied 3D Kirchhoff depth migration using conventional migration for UDD and mirror migration for DGD. A comparison of the migration results (Figure 4) shows a better image of both the seafloor and the shallow subsurface for the DGD result. Comparing the deeper subsurface (more than 400 m below the seafloor) the images of UDD and DGD are similar.

Discussion and Conclusions

UDD and DGD are now well-established components of the standard processing toolkit for multi-component seismic data. In this study, we have presented our implementations of UDD and DGD. We have demonstrated that DGD can be implemented with only minor modifications to the UDD processing flow. This process can improve the productivity compared to conventional processing of the downgoing wavefield, because only a single processing sequence is required for preparing the up- and downgoing wavefields for imaging.

The combination of UDD and DGD techniques is particularly attractive because it allows the construction of complimentary images from the up- and downgoing wavefields. For the shallow subsurface the DGD image is superior to the UDD image due to smaller reflection angles and the larger number of pre-critical input traces. Consequently, the combination of the two techniques may have great impact for the characterization of shallow targets.

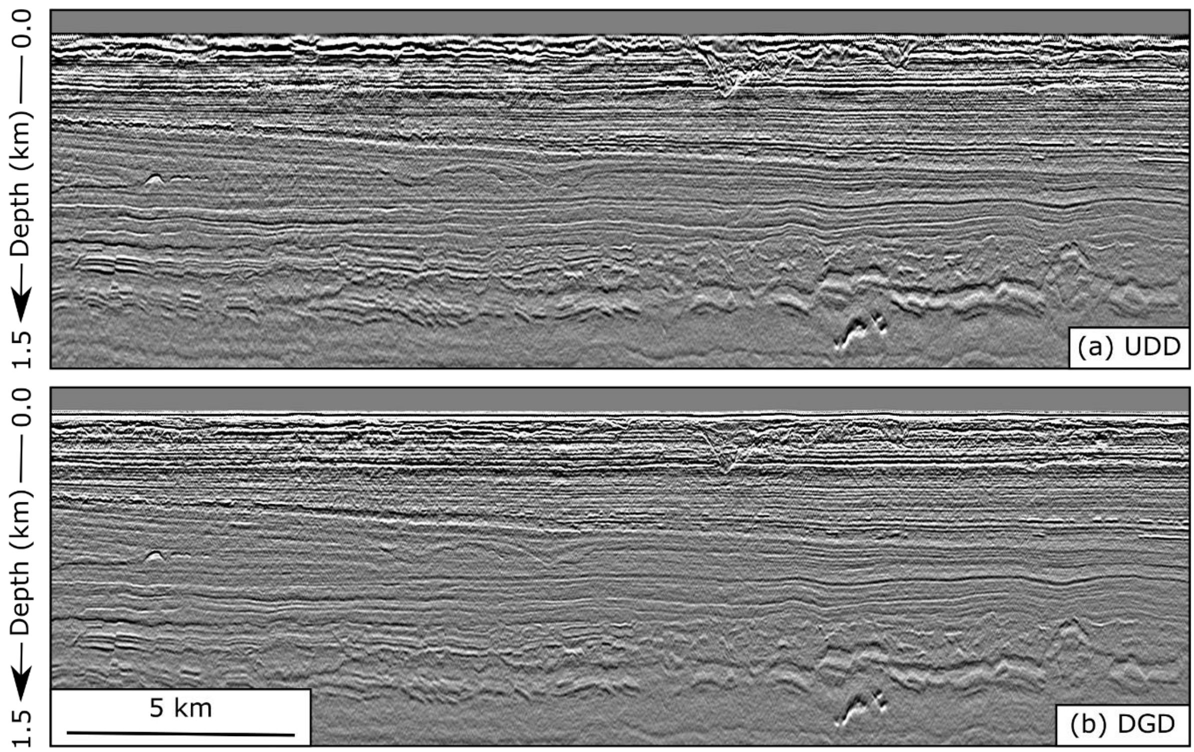

Figure 4 *Data example from the Utsira survey after Kirchhoff depth migration for the same data after UDD and DGD.*

Acknowledgements

This work was made possible through the support of TGS colleagues and management. We are thankful to Peter Lee and Bin Wang for their advice. Finally, we acknowledge AGS for acquisition of the survey.

References

Amundsen, L. [1993] Wavenumber-based filtering of marine point-source data. *Geophysics* **58**, 1335–1348.

Amundsen, L. [2020] Review of up-down deconvolution and multidimensional deconvolution for designature/free-surface demultiple of OBN seismic data. *SEG Technical Program Expanded Abstracts*, 3093–3098.

Caprioli, P. and Kristiansen, P. [2021] Data-driven prediction of downgoing free-surface multiples for ocean-bottom node data. *82nd EAGE Annual Conference & Exhibition*, 1–5.

Hampson, G. and Szumski, G. [2020] Down/Down Deconvolution. 82nd EAGE Annual Conference & Exhibition, 1–5.

Lokshtanov, D. [2005] Suppression of free-surface effects from multicomponent sea-floor data. *EAGE/SEG Research Workshop*, A01.

Lokshtanov, D. [2021] Fast and Efficient up-down Decomposition and Deconvolution for OBS Data, *82nd EAGE Annual Conference & Exhibition*, 1–5.

Sonneland, L. and Berg, L.E. [1987] Comparison of two approaches to water layer multiple attenuation by wave field extrapolation. *SEG Technical Program Expanded Abstracts*, 276–277.

Soubaras, R. [1996] Ocean bottom hydrophone and geophone processing. *SEG Technical Program Expanded Abstracts*, 24–27.

Wang, Y., Bale, R., Grion, S. and Holden, J. [2010] The ups and downs of ocean-bottom seismic processing: Applications of wavefield separation and up-down deconvolution. *The Leading Edge* **29**, 1258–1265.

Ziolkowski, A.M., Taylor, D.B. and Johnston, R.G.K. [1999] Marine seismic wavefield measurement to remove sea-surface multiples: Marine seismic wavefield measurement. *Geophysical Prospecting* **47**, 841–870.